Hindawi Publishing Corporation
International Journal of Photoenergy
Volume 2013, Article ID 890240, 6 pages
http://dx.doi.org/10.1155/2013/890240

Research Article

Photocatalytic Oxidation of Gaseous Benzene under 185 nm UV Irradiation

Haibao Huang,[1,2] Xinguo Ye,[1] Huiling Huang,[1] Peng Hu,[1] Lu Zhang,[1] and Dennis Y. C. Leung[3]

[1] *School of Environmental Science and Engineering, Sun Yat-Sen University, Guangzhou 510275, China*
[2] *Guangdong Provincial Key Laboratory of Environmental Pollution Control and Remediation Technology, Guangzhou 510275, China*
[3] *Department of Mechanical Engineering, The University of Hong Kong, Pokfulam Road, Hong Kong*

Correspondence should be addressed to Haibao Huang; seabao8@gmail.com and Dennis Y. C. Leung; ycleung@hku.hk

Received 19 July 2013; Accepted 11 August 2013

Academic Editor: Guisheng Li

Benzene is a toxic air pollutant and causes great harm to human being. Photocatalytic oxidation (PCO) has been frequently studied for benzene removal, however, its PCO efficiency is still very low and the photocatalysts are easy to be deactivated. To improve the efficiency and stability of PCO, UV lamps with partial 185 nm UV irradiation were used to activate photocatalysts (denoted as 185-PCO). Cobalt modified TiO_2 (Co-TiO_2) was developed to improve the PCO activity and eliminate ozone generated from 185 nm UV irradiation. Results show that benzene removal efficiency of PCO with 254 nm UV irradiation (denoted as 254-PCO) is only 2.1% while it was greatly increased to 51.5% in 185-PCO. 185-PCO exhibited superior capacity for benzene oxidation. In the 185-PCO process, much ozone was left in case of TiO_2 as photocatalysts while it can be nearly eliminated by 1% Co-TiO_2.

1. Introduction

With the rapid development of economy and the increase in population, massive volatile organic compounds (VOCs) are discharged from both industry (such as chemical, petrochemical, painting, and coating factories) and human activities [1, 2]. VOCs not only do great harm to the health of human being but also cause serious damage to the atmospheric environment. They can lead to atmospheric compound pollution and haze. The haze weather, which lasted for a long time in many cities of China in early 2013, had caused much trouble to local people. It is of great significance to control VOCs pollution.

Benzene is a representative VOC. It is very toxic and carcinogenic. Benzene is hard to be destructed by conventional technology due to its benzene ring. The methods of benzene removal include conventional ways such as adsorption [3, 4], catalytic combustion [5], and biological degradation [6] and emerging ways such as nonthermal plasma [7] and photocatalysis [8–10]. However, the application of these methods is greatly limited due to their inherent drawbacks such as high cost, deactivation, and byproducts [11–14].

PCO is one of the fastest developed technologies for VOCs control. The most widely used UV sources in PCO are 254 nm and 365 nm UV lamp. However, the conventional PCO process has disadvantages such as photocatalyst deactivation, recombination of electron-hole pair, and low efficiency [15]. In order to improve the efficiency and stability of PCO, UV lamps with partial 185 nm UV irradiation (denoted as 185-PCO) were used to activate photocatalysts [16–18]. 185 nm UV lamps cannot only irradiate photocatalyst but also generate active oxidants such as •O, •OH, and ozone. They are also facile, cheap, and energy efficient. Previous study showed that the toluene removal of 185-PCO is 7 times higher than that of PCO under 254 nm UV irradiation (denoted as 254-PCO), and no obvious deactivation was observed in the former [19]. However, massive ozone was residual at the outlet of photocatalytic reactor since TiO_2 had poor activity towards ozone decomposition. Ozone is a byproduct and it is harmful to the environment and the health of human being; meanwhile it is a strong oxidant and can be used to enhance the oxidation of pollutants.

Cobalt is a commonly used metal not only for TiO_2 doping but also as an active component of ozone decomposition

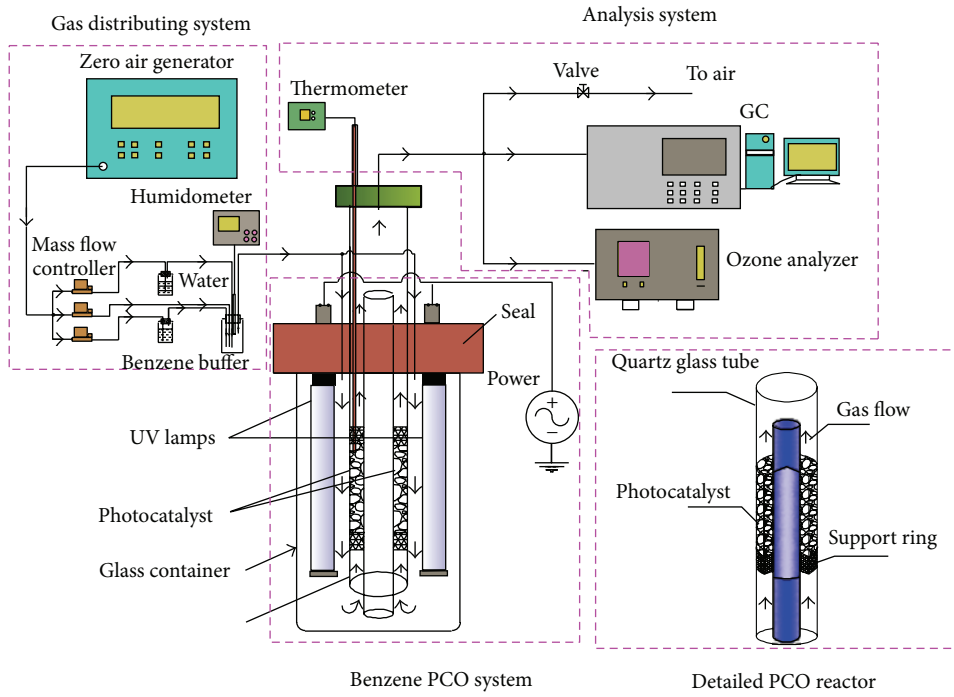

Figure 1: Schematic diagram of experimental setup.

agent. In this study, cobalt modified TiO_2 (Co-TiO_2) was developed to improve the PCO activity and eliminate ozone generated from 185 nm irradiation. Benzene was selected as representative VOC and its oxidation performance is compared between 185-PCO and 254-PCO. Results show that Co-TiO_2 can simultaneously increase benzene removal and ozone decomposition in 185-PCO. 185-PCO presents an efficient, economic, simple, and stable process for benzene removal.

2. Experimental Sections

2.1. Preparation of Photocatalysts. TiO_2 was prepared by sol-gel method using tetrabutyl titanate as the precursor, absolute alcohol as the solution, and HCl as the inhibitor, respectively. The preparation procedure is as follows: cobalt acetate was added into the mixture of 50 mL absolute alcohol and 17 mL tetrabutyl titanate and mixed for 30 min, forming solution A. Another mixture B containing 18 mL absolute alcohol, 1 mL HCl, and 3 mL deionized water was dropwise added into solution A under intensive stirring. The stirring was stopped till the gelatin was formed. The gelatin was aged for 12 h and then dried at 120°C for 6 h. The dry powder was followed by calcinations at 550°C for 4 h. Thus, cobalt doped TiO_2 was produced. Pure TiO_2 was fabricated by similar processes for the preparation of Co-TiO_2 except that no cobalt acetate was introduced during the synthesis. The catalysts were grinded into 40–60 mesh before use.

2.2. Catalytic Activity Test. The experimental setup and PCO reactor were shown in Figure 1. The catalytic activity test system was composed of 3 parts: gas distribution, benzene PCO, and gas analysis system. The gas from zero air generator is dry air free of CO, CO_2, and hydrocarbon. It was used for bubble water and benzene liquid to generate water and benzene vapor, respectively. The benzene concentration, humidity, and gas flow can be regulated by the mass flow controllers (S49, Horibametron). A 0.5 L/min gas flow of 50 ppm benzene concentration and 50% humidity was introduced into benzene PCO reactor. The reactor is a glass cylinder container with an effective volume of 0.5 L, in which a quartz glass tube was located in the centre and two UV lamps (4 W, Sungreen) were fixed in both sides of the tube with a distance of 8 mm. The detailed PCO reactor is shown in Figure 1. A solid rod of 8 mm diameter was placed in the center of the quartz glass tube with 1.3 cm i.d. and the photocatalysts was loaded in the space between the rod and glass tube. By this way, the photocatalysts have more chances to be irradiated by UV light. The UV lamps were turned on for 30 min for the warming-up of system before reaction and data recording. The gaseous benzene entered into the reactor from the bottom of glass tube and left from the top. The benzene and ozone concentrations of effluent were monitored by gas chromatography (GC) equipped with a FID (GC9790II, Fuli) and ozone analyzer (Model 202, 2B Technology) online, respectively.

2.3. Catalyst Characterization. BET surface areas of the samples were measured by N_2 adsorption-desorption isotherms at 77 K using Quadrasorb SI instrument. Prior to the measurement, the samples were degassed at 573 K for 2 h. The morphology of photocatalysts was obtained with scanning electron microscopy (SEM) (JSM-6330F, JEOL) operated at

Table 1: BET surface area of photocatalysts.

Samples	BET surface area, m^2/g	Particle size, nm
P25	55.4	29.0
TiO_2	96.6	10.5
Co-TiO_2	26.9	34.9

beam energy of 20.0 kV. XRD patterns were collected with a Panalytical Empyrean X-ray powder diffractometer operated at 35 kV and 25 mA, using Cu K α (λ = 1.5418 Å) radiation. The intensity data were collected in a 2θ range from 20° to 80°.

3. Results and Discussion

3.1. Characterization. Figure 2 shows the XRD spectra of the synthesized TiO_2 and Co-TiO_2 as well as the commercial TiO_2 (P25, Degussa). The nanocrystalline anatase structure was confirmed by (101), (004), (200), (105), and (204) diffraction peaks [20]. The XRD patterns of anatase have a main peak at 2θ = 25.2° corresponding to the 101 plane (JCPDS 21-1272) while the main peaks of rutile and brookite phases are at 2θ = 27.4° (110 plane) and 2θ = 30.8° (121 plane), respectively. Therefore, rutile and brookite phases have not been detected on the synthesized TiO_2 and Co-TiO_2. They exhibit very similar shape of diffractive peaks of the crystal planes. The XRD patterns did not show any Co phase, indicating that Co ions uniformly dispersed among the anatase crystallites. Unlike the synthesized TiO_2, weak peaks of rutile phase can be observed on P25 (Figure 1). The average particle size of TiO_2 was estimated by applying the Scherrer equation ($D = K\lambda/\beta \cos\theta$) on the anatase and rutile diffraction peaks (the most intense peaks for each sample), where D is the crystal size of the catalyst, λ is the X-ray wavelength (1.54 Å), β is the full width at half maximum (FWHM) of the catalyst (radian), K = 0.89, and θ is the diffraction angle [21]. The average crystal sizes of TiO_2, 1% Co-TiO_2, and P25 were calculated to be around 10.5 nm, 34.9 nm, and 29.0 nm, respectively, as shown in Table 1. Compared with P25, the synthesized TiO_2 can greatly reduce the particle size; however, the doping of cobalt triggered the aggregation of particle during the synthesis process, leading to the increase in particle size.

This observation is consistent with the results of BET surface area and the observation of SEM images. The BET surface area of TiO_2, 1% Co-TiO_2 and P25 is 96.6, 26.9 and 55.4 m^2/g, respectively. TiO_2 with the smallest particle size has the largest BET surface area.

SEM micrograph of TiO_2, 1% Co-TiO_2, and P25 nanoparticles is shown in Figure 3. This image shows uniform small particles which are coherent together on the TiO_2 and P25; however, the particles of 1% Co-TiO_2 got aggregated. The results agree well with the results of XRD pattern and BET surface area.

3.2. Catalytic Activity Test. Figure 4 compared benzene removal efficiency in PCO processes with 185 nm and 254 nm UV irradiation. It can be found that it is very low in case

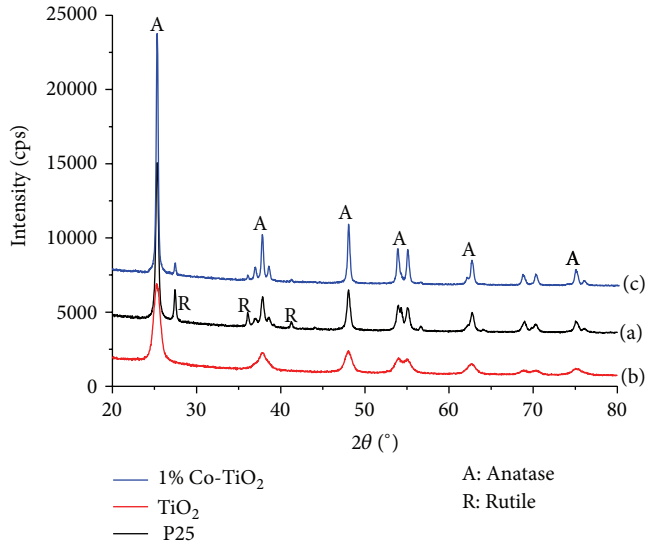

Figure 2: XRD spectra of photocatalysts: (a) P25, (b) TiO_2, and (c) 1% Co-TiO_2.

of 254-PCO process. Benzene removal efficiency is only about 2%. It is well known that benzene is very difficult to be destructed due to its stable π-bonding. Moreover, the intermediates from benzene PCO can lead to the serious deactivation of photocatalysts [22]. However, benzene conversion was greatly increased to about 50% under 185 nm UV irradiation and no obvious deactivation was observed after reaction for 3 h. Among 3 tested samples, Co-TiO_2 obtained the highest benzene removal efficiency of 51.5%, followed by P25 (50.2%) and TiO_2 (45.7%). Benzene removal efficiency of 185-PCO is over 20 times than that of 254-PCO. 185-PCO is a very complex process, in which 185 nm UV lamp not only acted as the irradiation light of photocatalysis but also generated reactive oxidants such as •O, •OH, and ozone. The reaction processes for the formation of reactive oxidants are as follows [23]:

$$\begin{aligned} H_2O + h\nu &\longrightarrow \bullet H + \bullet OH \\ O_2 + h\nu &\longrightarrow 2 \bullet O \\ \bullet O + H_2O &\longrightarrow 2 \bullet OH \\ \bullet O + O_2 &\longrightarrow O_3 \end{aligned} \quad (1)$$

In order to clarify the contribution of 185 nm irradiation, the photocatalysts were removed from the reactor. The new process is photolysis. It can be found that benzene removal efficiency reached 38% under 185 nm irradiation alone. 185 nm photolysis contributes much to benzene oxidation in the 185-PCO process. The sum of benzene removal efficiency due to PCO and 185 nm photolysis is about 40%, which is approximately 10% smaller than that of 185-PCO. This indicated that other factors were also involved in benzene oxidation in the 185-PCO process besides photolysis and PCO. As we know, ozone can be abundantly generated from 185 nm UV irradiation. The ozone concentration is 138 ppm in the absence of photocatalysts. Ozone is strong

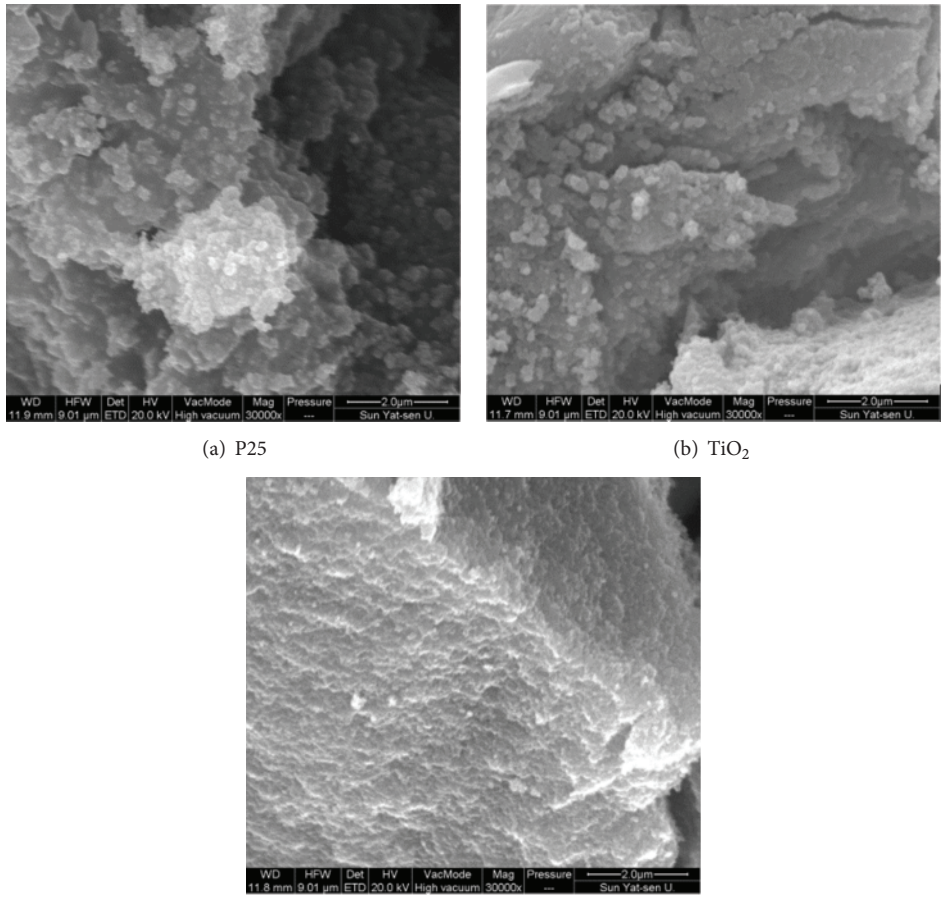

(a) P25 (b) TiO_2

(c) 1% Co-TiO_2

Figure 3: SEM images of photocatalysts: (a) P25, (b) TiO_2, and (c) 1% Co-TiO_2.

oxidant. Although it cannot directly oxidize benzene, it can be decomposed into more active oxygen species with the aid of catalysts [24]:

$$\begin{aligned} O_3 + {}^* &\longrightarrow O_2 + O^* \\ O^* + O_3 &\longrightarrow O_2 + O_2{}^* \\ O_2{}^* &\longrightarrow O_2 + {}^* \end{aligned} \quad (2)$$

* represents the catalytic active sites.

3.3. Ozone Decomposition. 185-PCO exhibited more superior capacity for benzene oxidation than 254-PCO. However, ozone is another important concern besides benzene removal since it is a toxic byproduct. Although 3 tested samples had similar benzene removal efficiency since 185 nm UV photolysis contributed to a large proportion of benzene removal, they had entirely different activity toward ozone decomposition. As shown in Figure 5, the ozone concentration at outlet of 185-PCO reactor after reaction for 2.5 h was 119 ppm in case of the synthesized TiO_2, and it was dropped to 58.4 ppm in case of P25. Although the synthesized TiO_2 had higher BET surface area than that of P25, its capacity for ozone decomposition is worse than that of the latter. It was reported that higher BET surface area should be helpful for ozone decomposition [25]. The difference between synthesized TiO_2 and commercial P25 is that the former is pure anatase

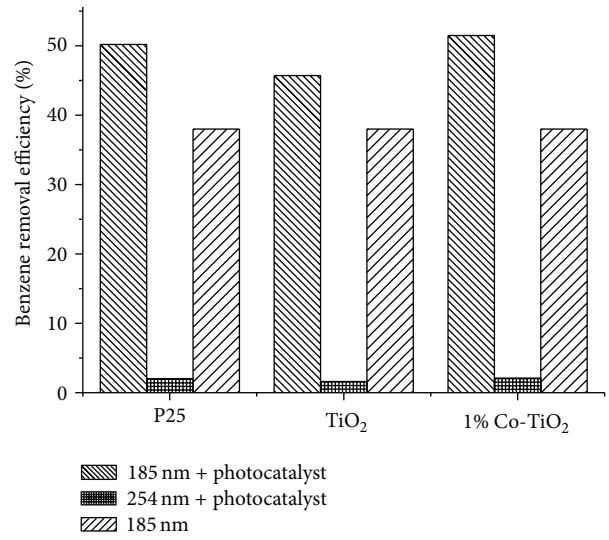

Figure 4: Benzene removal efficiency in different processes.

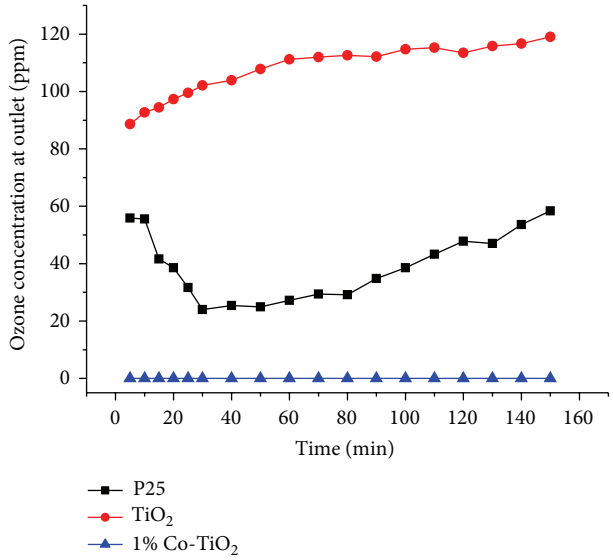

Figure 5: Ozone concentration at outlet of 185-PCO reactor with different photocatalysts.

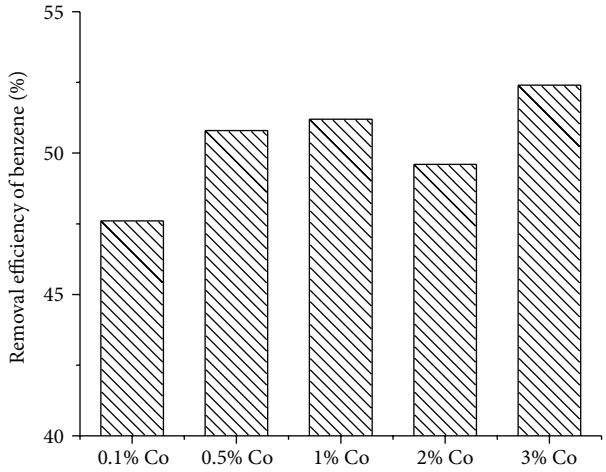

Figure 6: Effect of Co loading amount on benzene removal.

TiO_2 while P25 contained some rutile TiO_2 besides anatase one. A previous study showed that TiO_2 with partial rutile had better capacity for ozone decomposition than that of pure anatase TiO_2 [26]. As for Co-TiO_2, ozone can be completely eliminated. Cobalt is a very active component for ozone decomposition. Co doped TiO_2 exhibited superior activity toward ozone elimination. In comprehensive view of benzene removal and ozone decomposition, Co-TiO_2 exhibited the best performance among the 3 tested samples.

3.4. Effect of Co Doping. In order to study the effect of Co doping, 0.1%, 0.5%, 1%, 2%, and 3% Co-TiO_2 were prepared and tested in 185-PCO process. The results after reaction for 150 min are shown in Figure 6. Benzene removal efficiency is only 47.6% in case of 0.1% Co-TiO_2. As the increase in Co loading, benzene removal efficiency was increased to 51.5% in case of 1% Co-TiO_2 and 52.4% in case of 3% Co-TiO_2.

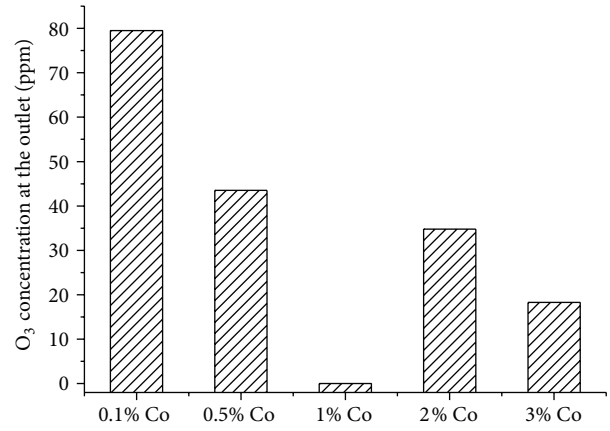

Figure 7: Effect of Co loading amount on ozone concentration at the outlet.

Figure 7 shows the effect of cobalt loading amount on ozone concentration at the outlet after reaction for 150 min. In case of Co doping amount lower than 1%, the ozone concentration at the outlet was dropped with the increase in Co loading. As for 0.1% Co doping, the ozone concentration is 79.5 ppm while it was decreased to nearly zero in case of 1% Co doping. The increase in Co doping can provide more catalytic active sites for ozone decomposition. However, the ozone concentration at the outlet was increased with further increase in Co doping. Too much Co doping is not beneficial to ozone decomposition since Co probably gets aggregated and blocks the micropore of TiO_2. This will reduce the catalytic active sites and BET surface area, leading to worse activities toward ozone decomposition.

4. Conclusion

To improve the efficiency and stability of PCO, 185-PCO was used to activate photocatalysts. Co-TiO_2 was developed to improve the PCO activity and eliminate the ozone generated from 185 nm UV irradiation. Results show that benzene removal efficiency of PCO with 254-PCO is only 2.1% while it was greatly increased to 51.5% in the 185-PCO process. 185 nm UV irradiation can generate much reactive oxygen species such as •O, •OH, and ozone, which can jointly enhance benzene oxidation together with PCO. In 185-PCO, much ozone is left in case of TiO_2 as photocatalysts while it can be completely eliminated by 1% Co-TiO_2. 185-PCO is an efficient and promising process for benzene removal.

Acknowledgments

The authors gratefully acknowledge the financial support from Research Fund for the Doctoral Program of Higher Education of China (no. 20120172120039), the National Nature Science Foundation of China (no. 51208207), the Research Fund Program of Guangdong Provincial Key Laboratory of Environmental Pollution Control and Remediation Technology (no. 2013K0001), and the Fundamental Research Funds for the Central Universities (no. 13lgzd03).

References

[1] R. Atkinson, "Atmospheric chemistry of VOCs and NO_x," *Atmospheric Environment*, vol. 34, no. 12–14, pp. 2063–2101, 2000.

[2] S. Zuo, F. Liu, J. Tong, and C. Qi, "Complete oxidation of benzene with cobalt oxide and ceria using the mesoporous support SBA-16," *Applied Catalysis A*, vol. 467, pp. 1–6, 2013.

[3] A. A. M. Daifullah and B. S. Girgis, "Impact of surface characteristics of activated carbon on adsorption of BTEX," *Colloids and Surfaces A*, vol. 214, no. 1–3, pp. 181–193, 2003.

[4] M. Farhadian, D. Duchez, C. Vachelard, and C. Larroche, "BTX femoval from polluted water through bioleaching processes," *Applied Biochemistry and Biotechnology*, vol. 151, no. 2-3, pp. 295–306, 2008.

[5] L. Wang, V. D. Vien, K. Suzuki, M. Sakurai, and H. Kameyama, "Preparation of anodised aluminium catalysts by an electrolysis supporting method for VOC catalytic combustion," *Journal of Chemical Engineering of Japan*, vol. 38, no. 2, pp. 106–112, 2005.

[6] G. Darracq, A. Couvert, C. Couriol, E. Dumont, A. Amrane, and P. Le Cloirec, "Activated sludge acclimation for hydrophobic VOC removal in a two-phase partitioning reactor," *Water, Air and Soil Pollution*, vol. 223, no. 6, pp. 3117–3124, 2012.

[7] M. Kang, B.-J. Kim, S. M. Cho et al., "Decomposition of toluene using an atmospheric pressure plasma/TiO_2 catalytic system," *Journal of Molecular Catalysis A*, vol. 180, no. 1-2, pp. 125–132, 2002.

[8] T.-C. Pan, H.-C. Chen, G.-T. Pan, and C.-M. Huang, "Photocatalytic oxidation of gaseous isopropanol using visible-light active silver vanadates/SBA-15 composite," *International Journal of Photoenergy*, vol. 2012, Article ID 314361, 8 pages, 2012.

[9] F.-L. Cao, J.-G. Wang, F.-J. Lv et al., "Photocatalytic oxidation of toluene to benzaldehyde over anatase TiO_2 hollow spheres with exposed 001 facets," *Catalysis Communications*, vol. 12, no. 11, pp. 946–950, 2011.

[10] A. Kachina, S. Preis, G. C. Lluellas, and J. Kallas, "Gas-phase and aqueous photocatalytic oxidation of methylamine: the reaction pathways," *International Journal of Photoenergy*, vol. 2007, Article ID 32524, 6 pages, 2007.

[11] S. K. Agarwal and J. J. Spivey, "Economic effects of catalyst deactivation during VOC oxidation," *Environmental Progress*, vol. 12, pp. 182–185, 1993.

[12] M. D. Driessen, T. M. Miller, and V. H. Grassian, "Photocatalytic oxidation of trichloroethylene on zinc oxide: characterization of surface-bound and gas-phase products and intermediates with FT-IR spectroscopy," *Journal of Molecular Catalysis A*, vol. 131, no. 1–3, pp. 149–156, 1998.

[13] M. Kosusko, "Catalytic oxidation of groundwater stripping emissions," *Environmental Progress*, vol. 7, no. 2, pp. 136–142, 1988.

[14] J. Jeong, K. Sekiguchi, W. Lee, and K. Sakamoto, "Photodegradation of gaseous volatile organic compounds (VOCs) using TiO_2 photoirradiated by an ozone-producing UV lamp: decomposition characteristics, identification of by-products and water-soluble organic intermediates," *Journal of Photochemistry and Photobiology A*, vol. 169, no. 3, pp. 279–287, 2005.

[15] H. B. Huang and D. Y. C. Leung, "Vacuum ultraviolet-irradiated photocatalysis: advanced process for toluene abatement," *Journal of Environmental Engineering*, vol. 137, no. 11, pp. 996–1001, 2011.

[16] J. Jeong, K. Sekiguchi, and K. Sakamoto, "Photochemical and photocatalytic degradation of gaseous toluene using short-wavelength UV irradiation with TiO_2 catalyst: comparison of three UV sources," *Chemosphere*, vol. 57, no. 7, pp. 663–671, 2004.

[17] L. Yang, Z. Liu, J. Shi, Y. Zhang, H. Hu, and W. Shangguan, "Degradation of indoor gaseous formaldehyde by hybrid VUV and TiO_2/UV processes," *Separation and Purification Technology*, vol. 54, no. 2, pp. 204–211, 2007.

[18] P. Zhang, J. Liu, and Z. Zhang, "VUV photocatalytic degradation of toluene in the gas phase," *Chemistry Letters*, vol. 33, no. 10, Article ID CL-040801, pp. 1242–1243, 2004.

[19] H. Huang, D. Y. C. Leung, G. Li, M. K. H. Leung, and X. Fu, "Photocatalytic destruction of air pollutants with vacuum ultraviolet (VUV) irradiation," *Catalysis Today*, vol. 175, no. 1, pp. 310–315, 2011.

[20] Y. Xie, S. H. Heo, S. H. Yoo, G. Ali, and S. O. Cho, "Synthesis and photocatalytic activity of anatase TiO_2 nanoparticles-coated carbon nanotubes," *Nanoscale Research Letters*, vol. 5, no. 3, pp. 603–607, 2010.

[21] M. Hamadanian, A. Reisi-Vanani, and A. Majedi, "Preparation and characterization of S-doped TiO_2 nanoparticles, effect of calcination temperature and evaluation of photocatalytic activity," *Materials Chemistry and Physics*, vol. 116, no. 2-3, pp. 376–382, 2009.

[22] H. Yuzawa, J. Kumagai, and H. Yoshida, "Reaction mechanism of aromatic ring amination of benzene and substituted benzenes by aqueous ammonia over platinum-loaded titanium oxide photocatalyst," *The Journal of Physical Chemistry C*, vol. 117, pp. 11047–11058, 2013.

[23] T. Alapi and A. Dombi, "Direct VUV photolysis of chlorinated methanes and their mixtures in an oxygen stream using an ozone producing low-pressure mercury vapour lamp," *Chemosphere*, vol. 67, no. 4, pp. 693–701, 2007.

[24] W. Li, G. V. Gibbs, and S. T. Oyama, "Mechanism of ozone decomposition on a manganese oxide catalyst—1. In situ Raman spectroscopy and Ab initio molecular orbital calculations," *Journal of the American Chemical Society*, vol. 120, no. 35, pp. 9041–9046, 1998.

[25] H. Huang, D. Ye, and X. Guan, "The simultaneous catalytic removal of VOCs and O_3 in a post-plasma," *Catalysis Today*, vol. 139, no. 1-2, pp. 43–48, 2008.

[26] H. Yin, J. Xie, Q. Yang, and C. Yin, "Mechanism of ozone decomposition on the surface of metal oxide," *Chemical Research and Application*, vol. 15, pp. 1–5, 2003.